RSC Advances

PAPER

View Article Online
View Journal | View Issue

Cite this: *RSC Adv.*, 2017, **7**, 44639

Sorption and sensing properties of coordination polymers with mixed 1,3,5-tri(1-imidazolyl)benzene and 2,6-naphthalenedicarboxylate ligands†

Ye Deng,[a] Zhao-Yu Yao,[a] Peng Wang,[a] Yue Zhao,[a] Yan-Shang Kang,[a] Mohammad Azam,[b] Saud I. Al-Resayes[b] and Wei-Yin Sun *[a]

Received 24th July 2017
Accepted 11th September 2017

DOI: 10.1039/c7ra08165k

rsc.li/rsc-advances

Under hydro/solvothermal conditions, the assembly of imidazole-containing ligand 1,3,5-tri(1-imidazolyl) benzene (tib) and 2,6-naphthalenedicarboxylic acid (H_2NDC) with different transition metal salts provides five new coordination polymers $[M_2(tib)_2(NDC)(H_2O)_2]$ $SO_4 \cdot XH_2O$ (**1**: M = Cd, X = 4; **2**: M = Co, X = 4; **3**: M = Ni, X = 3), $[Cd_2(tib)_2(NDC)(NO_3)_2]$ 2.5DMF·H_2O (**4**) (DMF = *N*,*N*-dimethylformamide) and $[Zn(tib)_{2/3}(NDC)]$ (**5**). **1–3** have the same three-fold interpenetrating 3D framework structures with SO_4^{2-} as counteranion, while **4** with NO_3^- as terminal ligand exhibits a wave-like 2D layer structure, which is further extended into a 3D framework by hydrogen bonds. In addition, complex **5** obtained at high temperature is an interesting two-fold interpenetrating 3D structure. Sorption and photoluminescence properties of the complexes were investigated. **4** displays selective adsorption of CO_2 over N_2. Furthermore, **1** and **4** can be used to probe acetone molecules selectively and rapidly *via* fluorescence quenching.

Introduction

Crystal engineering of coordination polymers (CPs) as well as metal–organic frameworks (MOFs) has been extensively studied in the past years, however, further systematic study is required for predictable and controllable synthesis of desired MOFs with specific properties and potential applications in gas storage/separation, catalysis, magnetism, photoluminescence and so on.[1] In recent years, MOFs have been developed and show perspective in molecular sensing and probes, particularly in monitoring harmful components in industrial and environmental fields as well as the active components in organisms.[2]

With respect to fluorescence sensing, lanthanide-MOFs have superiority benefitting from metal-based emissions.[3] In addition, some transition metal ions such as cadmium(II) ion has also been used to construct MOFs with sensing properties. For example, a porous three-dimensional (3D) MOF $[Cd(NDC)_{0.5}(PCA)]$ G_x (H_2NDC = 2,6-naphthalenedicarboxylic acid, HPCA = 4-pyridinecarboxylic acid, G = guest molecules) was synthesized by reaction of Cd(II) salt with H_2NDC and HPCA ligands, and can sensitively and selectively detect TNP (2,4,6-trinitrophenol) from mixed nitro explosives.[4] In 2014, another Cd-MOF CZJ-3 with formula of $[CdL(H_2O)]$ 4DMF·$2H_2O$ [H_2L = (*E*)-4-(2-carboxyvinyl)benzoic acid] has been reported. There are one-dimensional (1D) hexagonal nanotube channels in CZJ-3, which can absorb rhodamine B molecules to accomplish luminescent Rho@CZJ-3, as a result, sensing various volatile organic molecules can be easily realized by monitoring the photoluminescence of Rho@CZJ-3.[5] Furthermore, Cd-MOFs also made gratifying achievements in the aspect of ion sensing. A dual-emission 3D MOF $\{[Cd_{1.5}(EDDA)](H_3O)(H_2O)_3\}_n$ (H_4EDDA = 5,5′-[ethane-1,2-diylbis(oxy)]diisophthalic acid) has been recognized as the first example of MOF-implicated sensor for Hg(II) ions in water rapidly and sensitively.[6] There are some other luminescent Cd-MOFs based on carboxylate ligands that are applied to chemical sensing.[7] However, examples of imidazole-containing ligand based MOFs with sensing property are quite limited. In this work, we introduced rigid tripodal imidazole-containing ligand 1,3,5-tris(1-imidazolyl)benzene (tib) and dicarboxylic acid of 2,6-naphthalenedicarboxylic acid (H_2NDC) to react with different metal salts and five new MOFs, $[M_2(tib)_2(NDC)(H_2O)_2]$ $SO_4 \cdot XH_2O$ (**1**: M = Cd, X = 4; **2**: M = Co, X = 4; **3**: M = Ni, X = 3), $[Cd_2(tib)_2(NDC)(NO_3)_2]$ 2.5DMF·H_2O (**4**) (DMF = *N*,*N*-dimethylformamide) and $[Zn(tib)_{2/3}(NDC)]$ (**5**) were obtained. Selective gas sorption and sensing properties of the complexes were investigated and the Cd-MOFs were proved to be capable of sensing acetone molecules.

[a]*Coordination Chemistry Institute, State Key Laboratory of Coordination Chemistry, School of Chemistry and Chemical Engineering, Nanjing National Laboratory of Microstructures, Collaborative Innovation Center of Advanced Microstructures, Nanjing University, Nanjing 210023, China. E-mail: sunwy@nju.edu.cn*

[b]*Department of Chemistry, College of Science, King Saud University, P. O. Box 2455, Riyadh 11451, Saudi Arabia*

† Electronic supplementary information (ESI) available: crystallographic data, PXRD and TG data. CCDC 1564034–1564038. For ESI and crystallographic data in CIF or other electronic format see DOI: 10.1039/c7ra08165k

Experimental

Materials and methods

Ligand tib was prepared according to the previously published procedure,[8] and other commercially available chemicals were used as received. Elemental analyses (EA) for C, H and N were performed on a Perkin–Elmer 240C elemental analyzer at the analysis center of Nanjing University. IR spectra were measured on a Bruker Vector 22 FT-IR spectrometer by the KBr method. Powder X-ray diffraction (PXRD) measurements were made on a Bruker D8 Advance instrument using Cu Kα radiation (λ = 1.5418 Å). Thermogravimetric analyses (TGA) were carried out on a Mettler-Toledo (TGA/DSC1) thermal analyzer from 30 °C to 800 °C under nitrogen flow with a heating rate of 10 °C min^{-1}. Gas sorption tests were taken on a Belsorp-max volumetric gas sorption instrument. Photoluminescence spectra were recorded on a Perkin–Elmer LS 55 spectrofluorometer and xenon arc lamp acts as the light source.

Preparation of $[Cd_2(tib)_2(NDC)(H_2O)_2]$ $SO_4 \cdot 4H_2O$ (1)

A mixture of tib (27.6 mg, 0.10 mmol), $CdSO_4 \cdot 8/3H_2O$ (25.6 mg, 0.10 mmol), H_2NDC (21.6 mg, 0.10 mmol) and H_2O (6 ml) was sealed in a Teflon-lined stainless steel container and heated at 90 °C for 3 days. After being cooled to room temperature, colorless block crystals of **1** were obtained in 57% yield. Anal. calcd for $C_{42}H_{42}N_{12}O_{14}SCd_2$: C, 42.19; H, 3.54; N, 14.06%. Found: C, 42.11; H, 3.59; N, 14.11%. IR (KBr pellet, cm^{-1}): 3442 (w), 3105 (m), 1622 (s), 1551 (s), 1513 (vs), 1411 (s), 1355 (m), 1264 (s), 1096 (s), 1018 (s), 935 (m), 849 (m), 806 (m), 652 (m).

Preparation of $[Co_2(tib)_2(NDC)(H_2O)_2]$ $SO_4 \cdot 4H_2O$ (2)

Complex **2** was obtained by the same procedure used for preparation of **1** except that $CdSO_4 \cdot 8/3H_2O$ was replaced by $CoSO_4 \cdot 7H_2O$ (28.1 mg, 0.1 mmol). Purple block crystals of **2** were obtained in 66% yield. Anal. calcd for $C_{42}H_{42}N_{12}O_{14}SCo_2$: C, 46.33; H, 3.89; N, 15.44%. Found: C, 46.29; H, 3.86; N, 15.41%. IR (KBr pellet, cm^{-1}): 3392 (m), 1679 (m), 1614 (s), 1509 (vs), 1419 (s), 1357 (w), 1301 (m), 1249 (s), 1105 (vs), 1006 (w), 929 (w), 788 (m).

Preparation of $[Ni_2(tib)_2(NDC)(H_2O)_2]$ $SO_4 \cdot 3H_2O$ (3)

The title complex **3** was also isolated by the same procedure used for the preparation of **1** except that $NiSO_4 \cdot 6H_2O$ (26.3 mg, 0.1 mmol) was used instead of $CdSO_4 \cdot 8/3H_2O$. Green block crystals of **3** were obtained in 61% yield. Anal. calcd for $C_{84}H_{80}N_{24}O_{26}S_2Ni_4$: C, 47.13; H, 3.77; N, 15.70%. Found: C, 47.10; H, 3.74; N, 15.75%. IR (KBr pellet, cm^{-1}): 3419 (vs), 1618 (s), 1548 (m), 1508 (m), 1419 (s), 1307 (w), 1257 (m), 1089 (s), 1018 (m), 790 (w).

Preparation of $[Cd_2(tib)_2(NDC)(NO_3)_2]$ 2.5DMF·H_2O (4)

A mixture of tib (27.6 mg, 0.10 mmol), $Cd(NO_3)_2 \cdot 4H_2O$ (30.8 mg, 0.10 mmol), H_2NDC (21.6 mg, 0.10 mmol) and DMF (6 ml) was sealed in a Teflon-lined stainless steel container and heated at 90 °C for 3 days. After being cooled to room temperature, colorless block crystals of **4** were obtained in 55% yield. Anal. calcd for $C_{49.5}H_{49.5}N_{16.5}O_{13.5}Cd_2$: C, 45.17; H, 3.79; N, 17.56%. Found: C, 45.21; H, 3.75; N, 17.58%. IR (KBr pellet, cm^{-1}): 3421 (s), 1622 (vs), 1517 (s), 1407 (w), 1322 (w), 1263 (s), 1101 (s), 1082 (s), 1016 (m), 952 (w), 847 (w), 828 (m), 763 (m).

Preparation of $[Zn(tib)_{2/3}(NDC)]$ (5)

A mixture of tib (27.6 mg, 0.10 mmol), $ZnSO_4 \cdot 7H_2O$ (28.7 mg, 0.10 mmol), H_2NDC (21.6 mg, 0.10 mmol) and H_2O (6 ml) was sealed in a Teflon-lined stainless steel container and heated at 180 °C for 3 days. After being cooled to room temperature, colorless block crystals of **5** were obtained in 48% yield. Anal. calcd for $C_{22}H_{14}N_4O_4Zn$: C, 56.98; H, 3.04; N, 12.08%. Found: C, 56.81; H, 3.02; N, 12.11%. IR (KBr pellet, cm^{-1}): 3419 (m), 3131 (m), 1602 (s), 1554 (s), 1497 (s), 1397 (s), 1375 (s), 1328 (vs), 1235 (m), 1188 (m), 1076 (w), 1013 (m), 930 (w), 788 (s), 688 (m).

Crystal structure determination

Crystallographic data for **1–5** were collected on a Bruker Smart Apex II CCD single-crystal X-ray diffractometer with a graphite-monochromated Mo Kα radiation (λ = 0.71073 Å) at 293(2) K. Multi-scan absorption corrections were applied using the SADABS program.[9] All the structures were solved by direct methods using the SHELXS-2016 program of the SHELXTL package and refined by the full-matrix least-squares method using SHELXL-2016.[10] All the non-hydrogen atoms in the structures were refined on F^2 with anisotropic displacement parameters. Except those of water molecules, the hydrogen atoms were placed geometrically and refined isotropically according to the riding model. The hydrogen atoms of water molecules in **1–3** were found directly. The atom O5 in **1** is disordered in two positions, each with site occupancies of 0.5, the NDC^{2-} ligands in **1** and **5** are disordered in two positions with site occupancies of 0.786(6) and 0.214(6) for **1** and 0.814(4) and 0.186(4) for **5**, the naphthalene rings of NDC^{2-} in **2** and **3** are also disordered in two positions with site occupancies of 0.4 and 0.6 for **2**, and 0.5 and 0.5 for **3**. All the SO_4^{2-} anions in **1–3** are passed through by two-fold axes. The highly disordered solvent molecules in **4** are difficult to resolve and their contribution of densities was modeled using the SQUEEZE routine in software PLATON.[11] The definite chemical formula of **4** were obtained from the overall contribution of crystallographic, EA and TG data. The details of the crystal parameters, data collection and refinements for the complexes are summarized in Table 1, selected bond lengths and angles as well as hydrogen bonding data are listed in Tables S1 and S2,† respectively.

Results and discussion

Crystal structures of $[M_2(tib)_2(NDC)(H_2O)_2]$ $SO_4 \cdot XH_2O$ (1: M = Cd, X = 4; 2: M = Co, X = 4; 3: M = Ni, X = 3)

The results of crystallographic analysis show that **1–3** crystalize in monoclinic space group *C*2/*c* (Table 1) and have the same framework structures, thus only the structure of **1** is described in detail here. Cd1 in **1** is bounded by two chelate carboxylate oxygen atoms (O1, O2) from one NDC^{2-}, three nitrogen ones

Table 1 Crystal data and structure refinements for **1–5**

Compound	**1**	**2**	**3**	**4**	**5**
Formula	$C_{42}H_{42}N_{12}O_{14}SCd_2$	$C_{84}H_{84}N_{24}O_{28}S_2Co_4$	$C_{84}H_{80}N_{24}O_{26}S_2Ni_4$	$C_{49.5}H_{49.5}N_{16.5}O_{13.5}Cd_2$	$C_{22}H_{14}N_4O_4Zn$
M_r	1195.73	2177.59	2140.68	1316.35	463.74
Crystal system	Monoclinic	Monoclinic	Monoclinic	Triclinic	Trigonal
Space group	$C2/c$	$C2/c$	$C2/c$	$P\bar{1}$	$P\bar{3}$
a (Å)	23.6468(18)	22.802(2)	22.602(1)	13.572(5)	19.1253(9)
b (Å)	13.261(1)	13.5397(12)	13.646(1)	14.157(5)	19.1253(9)
c (Å)	17.991(2)	17.2991(15)	17.163(1)	19.505(8)	8.5716(8)
α (°)	90	90	90	93.398(11)	90
β (°)	126.758(1)	125.990(1)	125.812(1)	110.063(9)	90
γ (°)	90	90	90	90.003(10)	120
V (Å^3)	4519.9(8)	4321.4(7)	4292.7(4)	3513(2)	2715.2(4)
Z	4	2	2	2	6
D_c (g cm^{-3})	1.757	1.674	1.656	1.244	1.702
M (mm^{-1})	1.070	0.903	1.010	0.667	1.399
F (000)	2408	2240	2208	1332	1416
Reflections collected	12 400	14 338	11 888	20 724	14 072
Unique reflections	3984	3793	3798	12 316	3463
Goodness-of-fit	1.073	0.991	1.086	1.031	1.030
Final R indices $[I > 2\sigma(I)]^{a,b}$	$R_1 = 0.0212$	$R_1 = 0.0458$	$R_1 = 0.0379$	$R_1 = 0.1021$	$R_1 = 0.0357$
	$wR_2 = 0.0483$	$wR_2 = 0.1239$	$wR_2 = 0.1008$	$wR_2 = 0.2452$	$wR_2 = 0.0891$
R Indices (all data)	$R_1 = 0.0250$	$R_1 = 0.0587$	$R_1 = 0.0426$	$R_1 = 0.1494$	$R_1 = 0.0476$
	$wR_2 = 0.0502$	$wR_2 = 0.1353$	$wR_2 = 0.1044$	$wR_2 = 0.2695$	$wR_2 = 0.0941$

^{a} $R_1 = \sum||Fo| - |Fc||/\sum|Fo|$. ^{b} $wR_2 = |\sum w(|Fo|^2 - |Fc|^2)|/\sum|w(Fo)^2|^{1/2}$, where $w = 1/[\sigma^2(Fo^2) + (aP)^2 + bP]$. $P = (Fo^2 + 2Fc^2)/3$.

(N1, N3B, N5A) from three different tib ligands and one coordinated water molecule (Fig. 1a). The Cd–O and Cd–N bond lengths are in the range of 2.275(2)–2.431(3) Å and 2.2854(17)–2.3017(17) Å (Table S1†), respectively. Each tib acts as a tridentate ligand and coordinates with three Cd(II) atoms, and each Cd(II) in turn links three tib to generate a rhombic-like two-dimensional (2D) network (Fig. 1b) with $\{4\cdot10^2\}$ topology (Fig. 1c). Ligands NDC^{2-} join the adjoining 2D layers to attain a ladder-like 3D structure along a axis possessing two different kinds of channels with apertures of 14.1 and 9.9 Å (Fig. 1d). The large cavity allows other frameworks to interpenetrate each other to result in the final three-fold interpenetrating framework of **1** (Fig. 1e). Topologically, ligands tib and Cd1 can be simplified as 3- and 4-connected nodes and NDC^{2-} is treated just as linker, thus **1** can be regarded as a (3, 4)-connected 2-nodal 3D net with point (Schläfli) symbol of $\{4\cdot6\cdot8\}\{4\cdot6^2\cdot8\cdot10^2\}$ (Fig. 1f).[12]

Crystal structure of $[Cd_2(tib)_2(NDC)(NO_3)_2]$ 2.5DMF·H_2O (4)

When the reaction was carried out in DMF using $Cd(NO_3)_2\cdot4H_2O$ instead of $CdSO_4\cdot8/3H_2O$, complex **4** was isolated. As illustrated in Fig. 2a, both Cd1 and Cd2 are seven- coordinated with pentagonal bipyramid coordination geometry by three nitrogen atoms from three different tib, two oxygen ones from one chelate carboxylate group of NDC^{2-} and two other oxygen ones from coordinated NO_3^- anion. Each tib connects three Cd(II) to form an infinite 1D chain which is further connected by NDC^{2-} to compose the 2D network structure of **2** with nano-sized cavities of 13.57 × 10.85 Å^2 (Fig. 2b). The 2D layers finally extend to 3D supramolecular architecture through the C–H···O hydrogen bonds (Fig. 2c and Table S2†). It is noteworthy that in contrast to the counter anion of SO_4^{2-} in **1**, NO_3^-

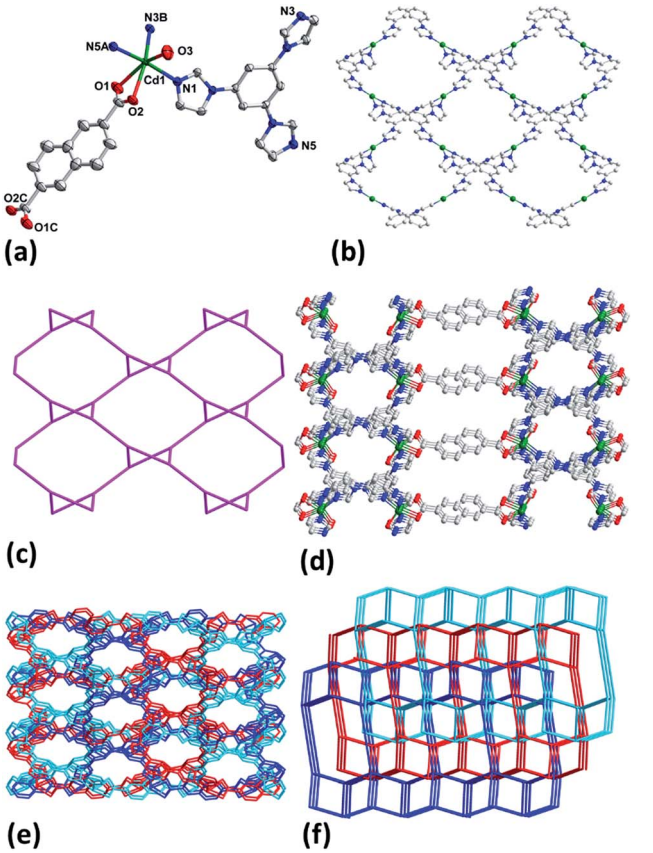

Fig. 1 (a) Coordination environment of Cd(II) in **1** with ellipsoids drawn at 30% probability level. The hydrogen atoms, free anion and water molecules are omitted for clarity. (b) 2D network of Cd-tib in **1**. (c) Topology of 2D Cd-tib in **1**. (d) 3D framework of **1**. (e) Interpenetrating 3D framework of **1**. (f) Topology of **1**.

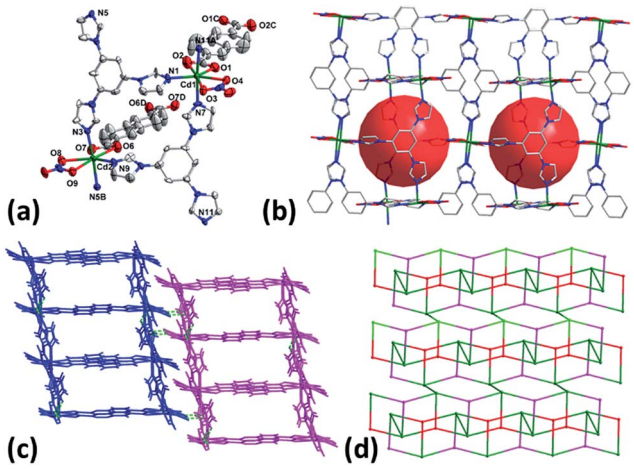

Fig. 2 (a) Coordination environment of Cd(II) in **4** with ellipsoids drawn at 30% probability level. The hydrogen atoms and free solvent molecules are omitted for clarity. (b) 2D layer of **4**. (c) 3D supramolecular architecture of **4**. (d) Topology of **4**.

acts as terminal ligand in **4**. The results imply that the anion plays important in determining the framework structures in this system.

From topological view, Cd1, Cd2 and tib can be viewed as 4-, 4- and 3-connected nodes and ditopic carboxylate NDC^{2-} acts as linker, leading to the formation of (3, 4)-connected 2-nodal 2D net with the point (Schläfli) symbol of $\{4^2\cdot6\}\{4^2\cdot6^3\cdot8\}$ (Fig. 2d).

Crystal structure of $[Zn(tib)_{2/3}(NDC)]$ (5)

When the reaction temperature was raised to 180 °C, complex **5** was obtained. Crystal structural analysis revealed that **5** crystalizes in trigonal space group $P\bar{3}$. The asymmetric unit of **5** contains one Zn(II), two thirds of tib and one NDC^{2-} ligand. It is noticeable that no coordinated or lattice solvent molecules were found in **5** thanks to the high reaction temperature.[13] Each Zn(II) in **5** is four-coordinated with distorted tetrahedral coordination geometry by two mono-dentate carboxylate oxygen atoms (O1, O4A) from two independent NDC^{2-} and two nitrogen ones (N1, N3) from two different tib ligands (Fig. 3a). It is worth noting that Zn(II) atoms link NDC^{2-} to present double helical chains along *b* axis (Fig. 3b) and ligands tib further connect helical chains to generate the 3D framework structure of **5** (Fig. 3c). The presence of large cavity in the framework leads to the formation of two-fold interpenetrating 3D net of **5** (Fig. 3e). By simplifying the tib and Zn(II) as 3- and 4-connected nodes, **5** also belongs to a (3,4)-connected 2-nodal 3D net with Schläfli symbol of $\{10^3\}_2\{10^6\}_3$ (Fig. 3d and f).

Powder X-ray diffraction (PXRD) and thermogravimetric analyses (TGA)

To ensure the phase purity of the bulk samples of **1–5** in the solid state, PXRD experiments were performed and the experimental patterns matched well with the simulated ones generated from the single crystal data (Fig. S1†), implying the pure phase of **1–5**. In addition, TGA were carried out to assess the

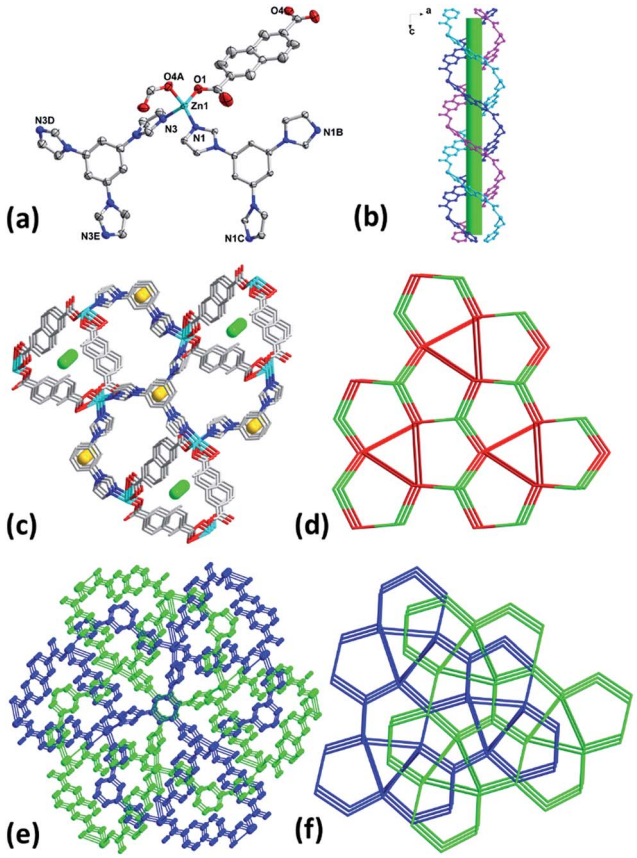

Fig. 3 (a) Coordination environment of Zn(II) in **5** with ellipsoids drawn at 30% probability level. The hydrogen atoms are omitted for clarity. (b) 1D double helical chains along *b* axis. (c) 3D framework with helical chains in **5**. (d) Topology of **5**. (e) Interpenetrating 3D framework of **5**. (f) Interpenetrating topology of **5**.

thermal stability of **1–5** and the results are exhibited in Fig. S2 and S3.† Complex **1** shows weight loss of 8.71% from room temperature to about 160 °C, which corresponds to the release of lattice and coordinated water molecules (calcd 9.03%). The decomposition of the framework occurred at 320 °C. For **2**, the weight loss of 9.64% (calcd 9.92%) between 30–210 °C is due to the loss of free and coordinated water molecules, and then the framework gradually decomposed above 300 °C. **3** loses 8.84% of its weight in the temperature range of 30–240 °C, which is attributed to the departure of three lattice and two coordinated water molecules (calcd 8.41%), and the residue is stable up to about 380 °C. For **4**, the weight loss of 16.65% (calcd 15.25%) between 30–235 °C corresponds to the loss of lattice water and DMF molecules, and then the framework gradually decomposed above 350 °C. **5** did not show obvious weight losses before the decomposition of the framework at about 300 °C, which is in agreement with the result of the crystal structural analysis.

Adsorption properties of 1 and 4

The porous structures of **1** and **4** discussed above suggested the possibility in the sorption aspect. Thus, the gas sorption properties of **1** and **4** were investigated. Acetone was used to

exchange the guest molecules inside the frameworks for 3 days and then the activation was carried out by heating the sample at 100 °C for 10 h under vacuum, the solvent molecules were completely removed without destroying the frameworks as confirmed by the PXRD and TG data (Fig. S1 and S2†).

As shown in Fig. 4, the sorption isotherm of **1** exhibits that only 4.80 $cm^3\ g^{-1}$ is adsorbed for N_2 at 77 K and 0.98 atm, while the CO_2 adsorption reaches 30.45 $cm^3\ g^{-1}$ (59.81 mg g^{-1}) at 195 K and 0.99 atm, corresponding to 1.5 CO_2 molecules per formula unit of **1**. The obvious hysteresis during desorption process of CO_2 in **1** can be attributed to the interaction of CO_2 molecules with framework of **1**. On the other hand, the CO_2 adsorption isotherm for **4** represents a typical type-I adsorption isotherm at 195 K as illustrated in Fig. 5.[14] The CO_2 uptake capacity of **4** is 73.19 $cm^3\ g^{-1}$ (143.77 mg g^{-1}) at 0.98 atm, amounting to 3.6 CO_2 molecules per formula unit of **4**. Similar to **1**, there is almost no adsorption of N_2 for **4** at 77 K. The selective sorption of CO_2 over N_2 for **1** and **4** implies the promising crystalline materials for separation of CO_2.[15]

Photoluminescence properties of 1, 4 and 5

CPs containing transition-metal ions without unpaired electrons, especially d^{10} metal ions, are advantageous candidates for luminescent materials.[16] Accordingly, the luminescent properties of free tib, **1**, **4** and **5** were examined in the solid state at room temperature. Intense emission band was observed at 415 nm for tib ligand with excitation at 360 nm, while emissions at 400 nm (λ_{ex} = 360 nm) for **1**, 429 nm (λ_{ex} = 365 nm) for **4** and 400 nm (λ_{ex} = 360 nm) for **5** were observed (Fig. 6). The blue shift of **1** as well as **5** can be assigned to the coordination of organic ligands with metal ions and interpenetrated 3D framework structures, while the red shift of emission observed in **4** may be attributed to the hydrogen bonding linked supramolecular structure. It has been reported that the crystal packing of the complex in the solid state has impact on their luminescence.[17]

It has been well established that a considerable amount of fluorescent MOF materials are sensitive to the presence of volatile organic molecules.[18] To examine whether **1**, **4** and **5** have abilities to detect small solvent molecules, each 5 mg fresh sample of **1**, **4** and **5** was immersed in 4 ml different organic solvent and it was found that only **1** and **4** are sensitive to the solvent molecules as evidenced by fluorescence intensity. The photoluminescence intensity of **1** and **4** depends on the identity of the solvent molecules with sequence of DMA > DMF > $CHCl_3$ > CH_2Cl_2 > THF > CH_3CN > EtOH > MeOH > acetone for **1** and DMF > DMA > CH_3CN > $CHCl_3$ > CH_2Cl_2 > THF > EtOH > MeOH > acetone for **4** (Fig. 7 and 8). It means that both **1** and **4** have significant quenching effect in the solvent of acetone, which can

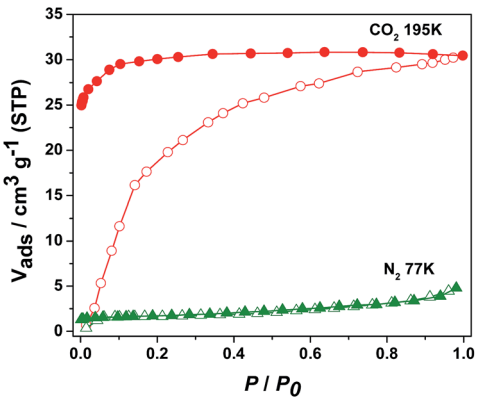

Fig. 4 N_2 (77 K) and CO_2 (195 K) adsorption isotherms of **1**.

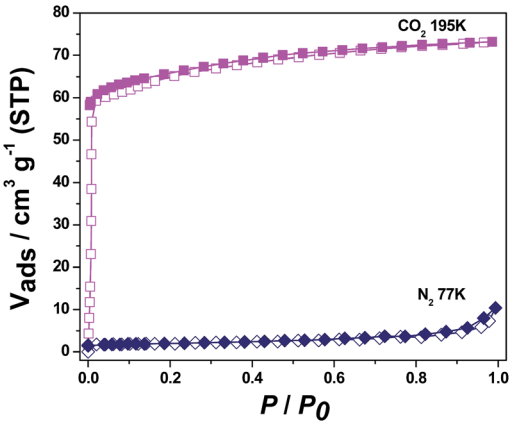

Fig. 5 N_2 (77 K) and CO_2 (195 K) adsorption isotherms of **4**.

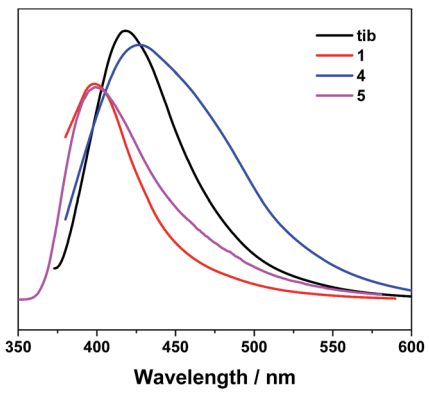

Fig. 6 Emission spectra of **1**, **4**, **5** and ligand tib in the solid state.

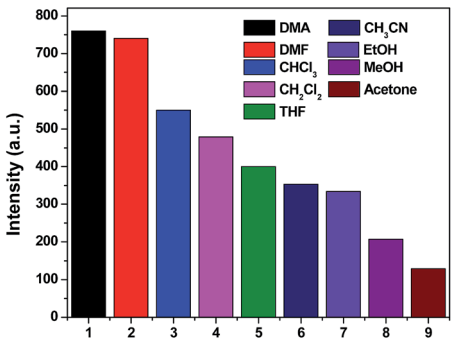

Fig. 7 Photoluminescence intensities of **1** in varied solvent when excited at 360 nm for **1**.

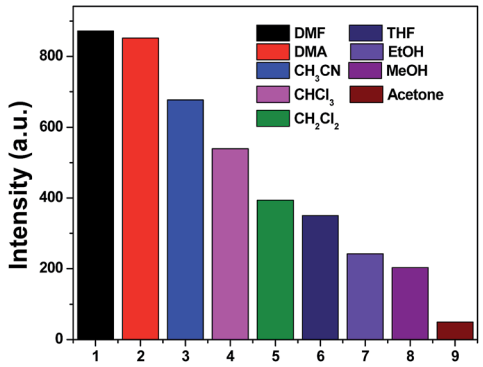

Fig. 8 Photoluminescence intensities of **4** in varied solvent when excited at 365 nm for **4**.

be attributed to the interactions between the framework and acetone molecule.[19]

To further explore the sensing sensitivity toward acetone, a collection of powder **1** and **4** immersed in DMA and DMF solution, respectively, quantitative acetone was gradually added to the solution. The invariable skeleton structures of **1** and **4** were ensured by the PXRD of **1** and **4** immersed in DMA/DMF/acetone (Fig. S1†). By monitoring the emission response, the fluorescence intensity decrease was observed with addition of acetone to the DMA and DMF emulsion of **1** and **4** (Fig. 9 and 11). The decreasing trend of the fluorescence intensity at 400 nm for **1** and 430 nm for **4** *vs.* the concentrations of acetone fitted well with a first-order exponential decay (Fig. 10 and 12), suggesting that fluorescence quenching of **1** and **4** by acetone are diffusion-controlled.[20] As a consequence, **1** and **4** can be potent candidates for acetone molecule sensing.

The results show that there are differences of the adsorption and luminescence properties of **1** and **4**, which may originate from their different framework structures. The large hysteresis and low adsorption capacity of CO_2 observed in **1** is caused by the presence of SO_4^{2-} counteranions, since SO_4^{2-} can interact with CO_2 but reduce the porosity of the framework. In addition, the varied hydrogen bonds within the solvent molecules and

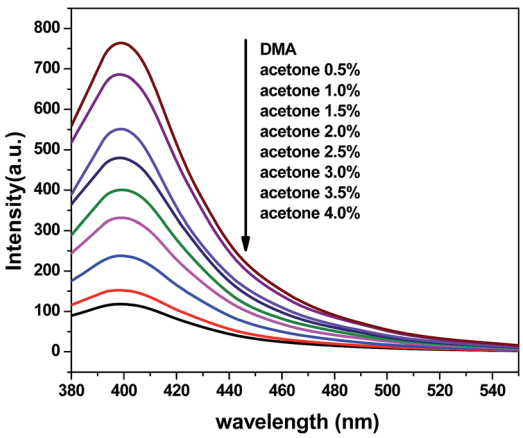

Fig. 9 Photoluminescence spectra of the dispersed **1** in DMA in the presence of different contents of the acetone solvent (excited at 360 nm).

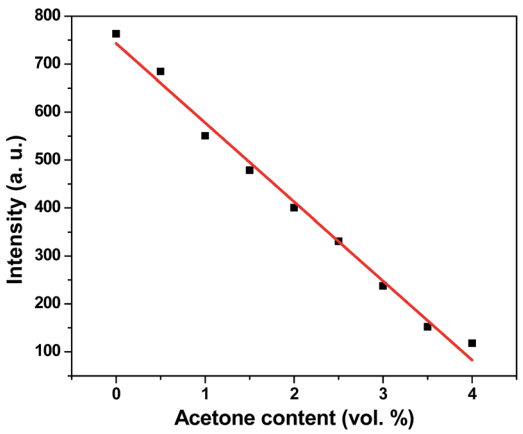

Fig. 10 Photoluminescence intensities of **1** in DMA as a function of acetone content.

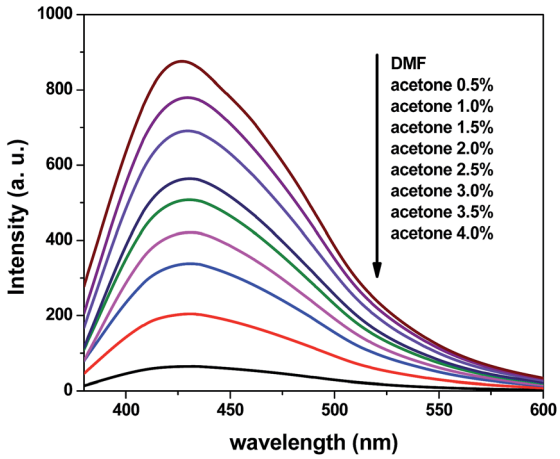

Fig. 11 Photoluminescence spectra of the dispersed **4** in DMF in the presence of different contents of the acetone solvent (excited at 365 nm).

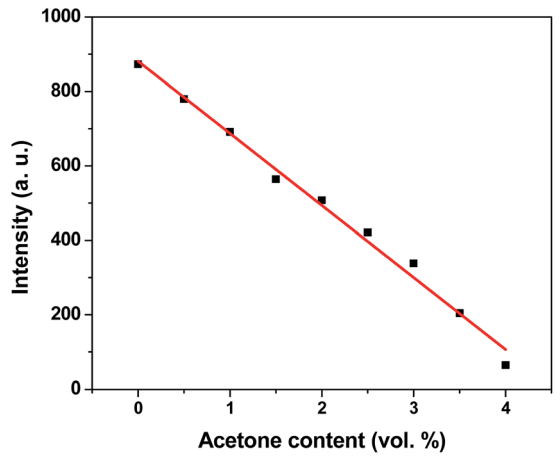

Fig. 12 Photoluminescence intensities of **4** in DMF as a function of acetone content.

skeleton of **4** may result in the different luminescence behavior from **1**.

Conclusions

Five coordination polymers with mixed organic ligands were synthesized under solvent thermal conditions. The results show that anions and reaction temperature play important role in the construction of frameworks. Adsorption experiments reveal that **1** and **4** can selectively adsorb CO_2 over N_2, in addition, both **1** and **4** can selectively and efficiently detect acetone molecules by fluorescence quenching *via* the interactions between the frameworks and acetone molecules, implying the application of CPs/MOFs in molecular sensing.

Conflicts of interest

There are no conflicts to declare.

Acknowledgements

This work was financially supported by the National Natural Science Foundation of China (grant no. 21331002 and 21573106). The authors extend their appreciation to the International Scientific Partnership Program ISPP at King Saud University for funding this research work through ISPP#0090. This work was also supported by a Project Funded by the Priority Academic Program Development of Jiangsu Higher Education Institutions.

Notes and references

1 (*a*) D. J. Tranchemontagne, J. L. Mendoza-Cortes, M. O'Keeffe and O. M. Yaghi, *Chem. Soc. Rev.*, 2009, **38**, 1257; (*b*) J. Y. Lee, O. K. Farha, J. Roberts, K. A. Scheidt, S. B. T. Nguyen and J. T. Hupp, *Chem. Soc. Rev.*, 2009, **38**, 1450; (*c*) O. K. Farha, I. Eryazici, N. C. Jeong, B. G. Hauser, C. E. Wilmer, A. A. Sarjeant, R. Q. Snurr, S. T. Nguyen, A. Ö. Yazaydın and J. T. Hupp, *J. Am. Chem. Soc.*, 2012, **134**, 15016; (*d*) Y.-J. Cui, Y.-F. Yue, G.-D. Qian and B.-L. Chen, *Chem. Rev.*, 2012, **112**, 1126; (*e*) P. Ramaswamy, N. E. Wong and G. K. H. Shimizu, *Chem. Soc. Rev.*, 2014, **43**, 5913; (*f*) Y.-Q. Huang, Y. Wan, H.-Y. Chen, Y. Wang, Y. Zhao and X.-F. Xiao, *New J. Chem.*, 2016, **40**, 7587; (*g*) Y.-Q. Huang, H.-D. Cheng, H.-Y. Chen, Y. Wan, C.-L. Liu, Y. Zhao, X.-F. Xiao and L.-H. Chen, *CrystEngComm*, 2015, **17**, 5690; (*h*) Z.-G. Gu, C.-H. Zhan, J. Zhang and X.-H. Bu, *Chem. Soc. Rev.*, 2016, **45**, 3122; (*i*) H.-R. Fu, Z.-X. Xu and J. Zhang, *Chem. Mater.*, 2015, **27**, 205.

2 (*a*) X. Du, R.-Q. Fan, X.-M. Wang, G.-Z. Yu, L.-S. Qiang, P. Wang, S. Gao and Y.-L. Yang, *Cryst. Growth Des.*, 2016, **16**, 1737; (*b*) Y.-L. Hou, H. Xu, R.-R. Cheng and B. Zhao, *Chem. Commun.*, 2015, **51**, 6769; (*c*) Z.-C. Hu, B. J. Deibert and J. Li, *Chem. Soc. Rev.*, 2014, **43**, 5815; (*d*) G. Férey, C. Mellot-Draznieks, C. Serre, F. Millange, J. Dutour, S. Surblé and I. Margiolaki, *Science*, 2005, **309**, 2040; (*e*) X.-J. Zhang, W.-J. Wang, Z.-J. Hu, G.-N. Wang and K. Uvdal, *Coord. Chem. Rev.*, 2015, **284**, 206.

3 (*a*) J. Sahoo, R. Arunachalam, P. S. Subramanian, E. Suresh, A. Valkonen, K. Rissanen and M. Albrecht, *Angew. Chem., Int. Ed.*, 2016, **55**, 9625; (*b*) W. Liu, T. Jiao, Y. Li, Q. Liu, M. Tan, H. Wang and L. Wang, *J. Am. Chem. Soc.*, 2004, **126**, 2280; (*c*) B. Chen, Y. Yang, F. Zapata, G. Lin, G. Qian and E. B. Lobkovsky, *Adv. Mater.*, 2007, **19**, 1693; (*d*) C. Zhan, S. Ou, C. Zou, M. Zhao and C.-D. Wu, *Anal. Chem.*, 2014, **86**, 6648; (*e*) J.-X. Ma, X.-F. Huang, X.-Q. Song and W.-S. Liu, *Chem.–Eur. J.*, 2013, **19**, 3590.

4 S. S. Nagarkar, B. Joarder, A. K. Chaudhari, S. Mukherjee and S. K. Ghosh, *Angew. Chem., Int. Ed.*, 2013, **52**, 2881.

5 M. J. Dong, M. Zhao, S. Ou, C. Zou and C.-D. Wu, *Angew. Chem., Int. Ed.*, 2014, **53**, 1575.

6 P.-Y. Wu, Y.-H. Liu, Y. Liu, J.-R. Wang, Y. Li, W. Liu and J. Wang, *Inorg. Chem.*, 2015, **54**, 11046.

7 (*a*) Y. Rachuri, B. Parmar, K. K. Bishta and E. Suresh, *Dalton Trans.*, 2016, **45**, 7881; (*b*) L. Li, C.-X. Li, Y.-L. Ren, M. Song, Y. Ma and R.-D. Huang, *CrystEngComm*, 2016, **18**, 7787; (*c*) M. M. Wanderley, C. Wang, C.-D. Wu and W. Lin, *J. Am. Chem. Soc.*, 2012, **134**, 9050; (*d*) Q.-K. Liu, J.-P. Ma and Y.-B. Dong, *Chem. Commun.*, 2011, **47**, 7185.

8 J. Fan, W.-Y. Sun, T. Okamura, W.-X. Tang and N. Ueyama, *Inorg. Chem.*, 2003, **42**, 3168.

9 G. M. Sheldrick, *SADABS*, University of Göttingen, Göttingen, Germany, 2003.

10 (*a*) G. M. Sheldrick, *SHELXS-2016, Program for the crystal structure solution*, University of Göttingen, Göttingen, Germany, 2016; (*b*) G. M. Sheldrick, *SHELXL-2016, Program for the crystal structure solution*, University of Göttingen, Göttingen, Germany, 2016.

11 (*a*) A. L. Spek, *Acta Crystallogr., Sect. B: Struct. Sci.*, 1990, **46**, 194; (*b*) A. L. Spek, *J. Appl. Crystallogr.*, 2003, **36**, 7.

12 V. A. Blatov, *TOPOS, A Multipurpose Crystallochemical Analysis with the Program Package*, Samara State University, Russia, 2009.

13 Y. Deng, P. Wang, Y. Zhao, Y.-S. Kang and W.-Y. Sun, *Microporous Mesoporous Mater.*, 2016, **227**, 39.

14 Y.-L. Li, D. Zhao, Y. Zhao, P. Wang, H.-W. Wang and W.-Y. Sun, *Dalton Trans.*, 2016, **45**, 8816.

15 H.-Y. Zhang, R.-L. Guo, J.-P. Hou, Z. Wei and X.-Q. Li, *ACS Appl. Mater. Interfaces*, 2016, **8**, 29044.

16 (*a*) F. Gandara, A. Andres, B. Gomez-Lor, E. Gutierrez-Puebla, M. Iglesias, M. A Monge, D. M. Proserpio and N. Snejko, *Cryst. Growth Des.*, 2008, **8**, 378; (*b*) Y. Zhou and B. Yan, *Nanoscale*, 2015, **7**, 4063; (*c*) Y. Lu and B. Yan, *Chem. Commun.*, 2014, **50**, 15443.

17 (*a*) R.-B. Fu, S.-C. Xiang, S.-M. Hu, L.-S. Wang, Y.-M. Li, X.-H. Huang and X.-T. Wu, *Chem. Commun.*, 2005, 5292; (*b*) Y.-Q. Huang, B. Ding, H.-B. Song, B. Zhao, P. Ren, P. Cheng, H.-G. Wang, D.-Z. Liao and S.-P. Yan, *Chem. Commun.*, 2006, 4906; (*c*) G.-Z. Liu, S.-H. Li, X.-L. Li, L.-Y. Xin and L.-Y. Wang, *CrystEngComm*, 2013, **15**, 4571; (*d*) J.-A. Hua, Y. Zhao, Q. Liu, D. Zhao, K. Chen and W.-Y. Sun, *CrystEngComm*, 2014, **16**, 7536; (*e*) Q. Hua,

Y. Zhao, G. C. Xu, M. S. Chen, Z. Su, K. Cai and W.-Y. Sun, *Cryst. Growth Des.*, 2010, **10**, 2553.

18 (*a*) X.-P. Wang, L.-L. Han, Z. Wang, L.-Y. Guo and D. Sun, *J. Mol. Struct.*, 2016, **1107**, 1; (*b*) J.-A. Hua, Y. Zhao, Y.-S. Kang, Y. Lu and W.-Y. Sun, *Dalton Trans.*, 2015, **44**, 11524.

19 C. A. Bauer, T. V. Timofeeva, T. B. Settersten, B. D. Patterson, V.-H. Liu, B. A. Simmons and M. D. Allendorf, *J. Am. Chem. Soc.*, 2007, **129**, 7136.

20 W. Yang, J. Feng and H. Zhang, *J. Mater. Chem.*, 2012, **22**, 6819.